Analysis of single cells treated with the KRAS[G12D] inhibitor MRTX 1133 reveals new challenges for the emerging field of single cell proteomics

Benjamin C. Orsburn[*]

The Department of Pharmacology and Molecular Sciences
Single Cell Proteomics Center
The Johns Hopkins University School of Medicine, Baltimore, MD, USA, 21205
[*]Corresponding: borsbur1@jhmi.edu

Abstract
Mutations in KRAS are common drivers of human cancers and are often those with the poorest overall prognosis for patients. A recently developed compound, MRTX1133 has shown promise in inhibiting the KRAS[G12D] mutant protein, which is a primary driver mutation in pancreatic cancer cases worldwide. In this study, I performed a multi-omic analysis of four cancer cell lines following acute treatment with this compound. To obtain increased granularity in the observed proteomic observation, I attempted to perform multiplexed single cell proteomics on all four cell lines with a goal of over 500 single cells per treatment condition. Due to a high level of cellular death and morphological changes induced in the two mutant cell lines following drug treatment, only two cell lines could be analyzed with this approach. The final results provided in this draft contain results from approximately 1,800 single cells from two cell lines which each harbor two copies of the KRAS[G12D] mutant gene. From these files 3,140 total proteins were identified with approximately 953 proteins quantified per cell. These results were sufficient to differentiate between single pancreatic cancer cells derived from different patients. In addition, I present observations suggesting new challenges to consider in pharmacological applications for single cell proteomics, including biases related to how the carrier channels are prepared and how single cells are selected or aliquoted. By sorting for viable cells following drug treatment that leads to high levels of cell death, I obtain very different results than when the entire populations are homogenized for bulk proteomics. These results suggest new questions for the application of single cell proteomics, and perhaps proteomics itself, when studying drug treatments that can result in diverse cellular responses including high cell death. All mass spectrometry data and processed results are publicly available via ProteomeXchange at accessions PXD039597, PXD039601 and PXD039600.

Abstract Graphic
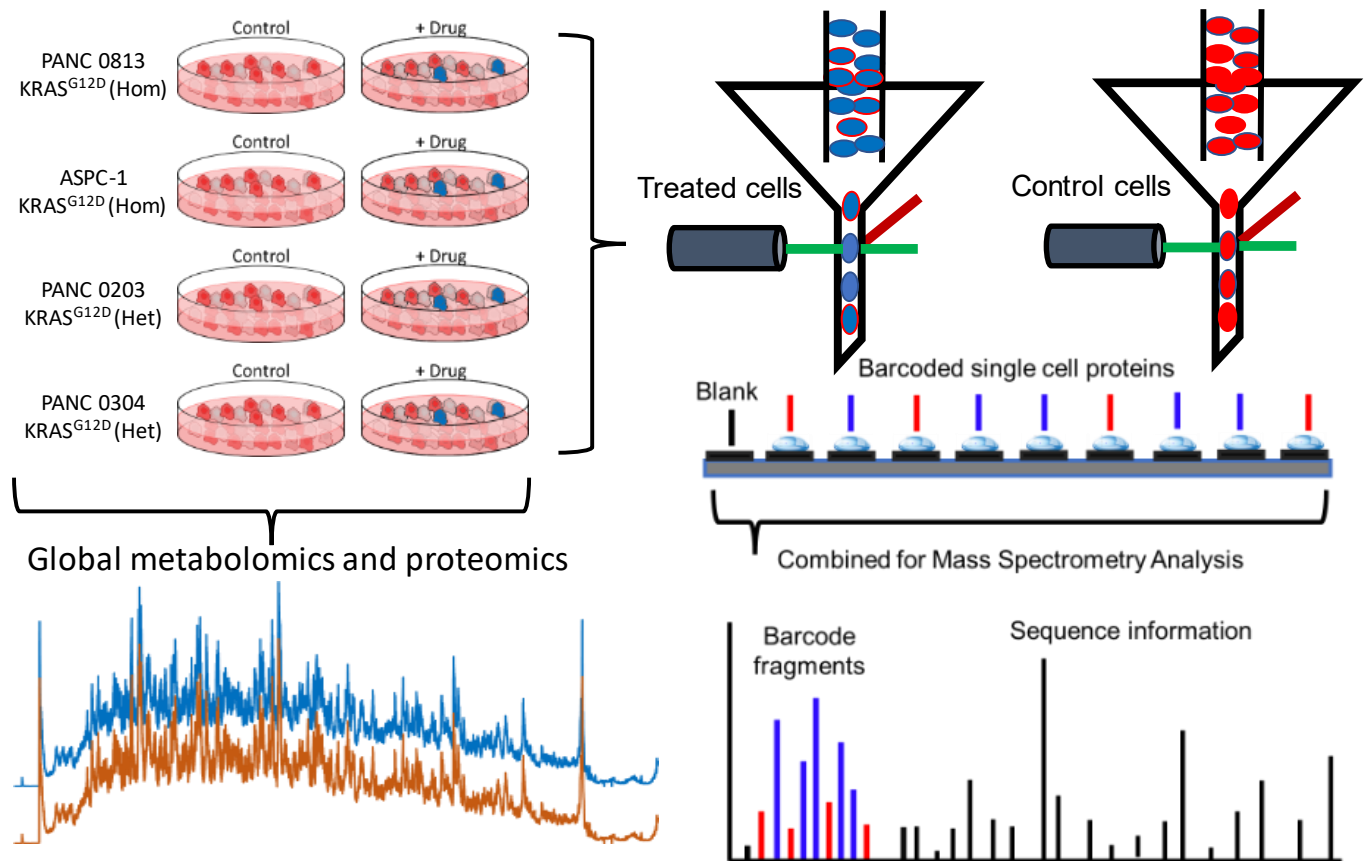
Introduction

KRAS mutations are found in up to 25% of solid tumors, and typically those with the worst prognosis.[1,2] A recently described compound MRTX1133 builds on the work of recent successes with KRAS small molecule inhibitors, as the first inhibitor described for KRAS[G12D] mutant cell lines.[3] MRTX1133 differs from successful KRASG12C inhibitors in that it does not bind covalently. Our primary concern was that without covalent binding, this new drug would lack biological efficacy and our work focused on using it as a model for single cell proteomic method development. However, recent work demonstrated the high effectiveness of MRTX1133 in both cell lines and xenograft mouse models, justifying a full functional study of this compound.[4,5]

We recently described the use of single cell proteomics to better attempt to better understand the heterogeneity of response in the proteomes of cells treated with a KRAS[G12C] inhibitor.[6] While more of a proof of concept, that study led to the development of tools for the application of multiplexed single cell proteomics using a TIMSTOF mass analyzer. Multiple limitations existed in that study, including the relatively small number of cells that were analyzed. We were, however, able to recapitulate many of the findings of both recent bulk proteomic and single cell transcriptomic studies of this drug while highlighting new findings that were not revealed by others. Following a year of heavy optimization to alleviate bottlenecks on the sample preparation and data analysis side, I have applied the resulting pipeline to the study of the acute cellular response of four cancer cell lines to MRTX1133. Bulk cell proteomics and

metabolomics were performed on these lines as a matter of standard practice in our lab prior to single cell analysis.

Results and Discussion

Metabolomics demonstrates ATP and NAD precursor depletion in all cell lines following MRTX 1133 treatment

Global reversed phase positive metabolomics identified 940 distinct small molecules after standard adduct reduction processes. Of these, 781 could be assigned a putative molecular formula and 264 could be assigned a putative identification within the cutoffs uses for this study (**Supplemental Data 1**). Principal component analysis (**Figure 1A**) suggests a level of uniformity following drug treatment greater than the control cell lines on their own. It is worth noting, however, that MRTX1133 ionizes particularly well, forming both a single and doubly charged molecular ion with extremely high efficiency (molecular weight; 600.2548, **Supplemental Data 1**). Due to these high signals, it is possible that this clustering is driven by the presence and absence of the drug itself in these lines. At a metabolomic level the most striking changes were that drug treatment revealed a universal depletion of ATP precursors in all cell lines following MRTX1133 treatment. Notably, adenosine, AMP and ADP were observed at reduced relative areas (**Figure 1B**). Nicotinamide and NAD+ were likewise reduced in all lines following treatment (**Figure 1C**). While subtle differences in the metabolomic profiles were observed in all cell lines following treatment, cell lines harboring single or double copies of the mutant gene differed in response in multiple cases, most notably in the levels of some amino acids such as glutamine. Cell lines with single copies of the KRAS[G12D] mutation appeared to demonstrate marked increases in glutamine levels following treatment while homozygous cell lines demonstrated slight decreases in concentration (**Figure 1D**).
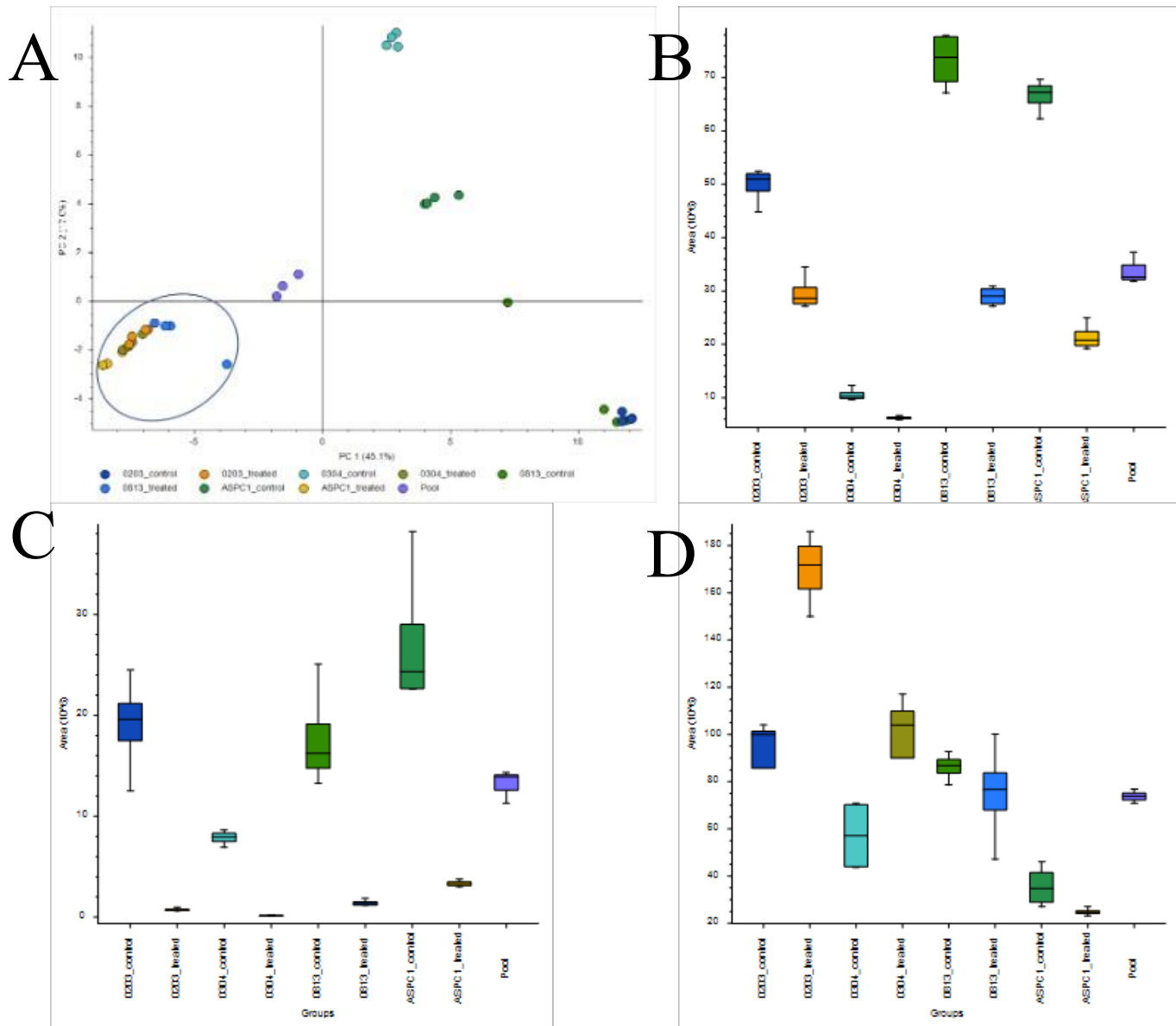
Figure 1. Representation of global metabolomic alterations following MRTX1133 treatment. A. A PCA plot demonstrating pronounced clustering of all cell lines following MRTX1133 treatment (circled) **B.** Adenine levels in each cell line are markedly reduced in all cell lines following treatment. **C.** The same trend is observed in AMP. **D.** Glutamine levels following treatment indicate a reversed effect in heterozygous and homozygous cell lines.

Proteomic bulk cell homogenate data

The bulk cell proteomics data largely produced expected changes in all cell lines. MRTX1133 acute treatment resulted in a consistent decrease in abundance in the central MAPK pathway. ERK (MAPK3) was most notably reduced in all cell lines following treatment, as previously reported[4] (**Supplementary Figure 1**). SimpliFi pathway analysis identified the Rho GTPase pathway as the seventh most significantly altered pathway between control and treated lines (R-HAS-563220; 2.04 x 10^{-60}). Similarly, MAPK was the 9th most

significant altered pathway (R-HSA-5687128; 7.41 x 10^{-53}). The MHC Class II antigen presentation system fell (R-HSA-2132295; 9.03 x 10^{-60} between these two pathways which is also somewhat expected based on work demonstrating high levels of MHC level expression in KRAS mutant cells.[7]

Single cell proteomics summary

We have recently described the use of a TIMSTOF mass spectrometer for SCoPE-MS single cell proteomics applications.[6] While we determined that higher loading channel concentrations could be utilized with little decrease in quantitative accuracy, they came at the expense of increased missing values. In this study I employed a protocol more similar to the original SCoPE-MS study in which 200 single cells from each condition were used for the loading channel in most experiments. By simply mixing the loading channels from each experimental condition and through the use of a pseudo-random mixing and loading protocol, I can combine SCP samples from multiple conditions within each LCMS experiment. Despite the reduced carrier channel of approximately 41.6ng of starting protein from each well, I obtained similar numbers to our previous work with approximately 953 proteins identified per cell when using a single search engine. Over the course of the study, a total of 3,143 protein groups were identified. We've found that the use of multiple search engines with false discovery estimation through a single instance of Percolator can lead to more than a twenty percent increase in identifications over a single search engine alone. In addition, multiple advanced tools for single cell analysis such as isobaric tag enabled match between runs [8], and posterior error adjustment can lead to a further increase in total identification rates.[9] These, however, take considerable time and effort to execute and are outside of the goals of this current study. The complete report of all proteins and quantification values for all single cells are provided as **Supplemental File 3**).

Standard proteomics tools can handle over 2,000 single cells

One question that arose from our previous study was in the capabilities of standard proteomic informatic tools to handle single cell proteomics data at increasing scale. In this study I've exclusively used the SequestHT search tool and Percolator within the commercial release of Proteome Discoverer 2.4 SP1. While the output file from this manuscript was challenging to manipulate at 126 gigabytes (GB), data visualization and filtering were possible on a desktop PC tower with 32 processing cores and 64 GB of RAM. Similarly, Perseus had no difficulty manipulating this entire dataset for analysis, including when employing non-linear dimensionality reduction such at U-MAP analysis through the Perseus R toolkit.[10]

Protein post translational modifications can be readily identified in all single cells that pass QC filters

As previously reported for the H358 cell line, I can easily detect and quantify multiple classes of protein PTMs in all cells analyzed in this study. The most abundant and readily observed PTMs are histone modifications, particularly the well characterized and tryptically convenient K28 and K80 lysine modification sites. **Figure 2** is a bar plot demonstrating the abundance of the K28 methylated and demethylated peptides. The former is the most commonly observed with signal in 75.8% (440/580) of the PANC 0813 single cells shown. When considering the possibility of methylation and dimethylation occupying the K28 site, 98.7% of single 0813 cells (573/580) demonstrate quantifiable signal. These results are similar throughout the study (data not shown). As we have previously observed, the ability to detect protein PTMs is directly related to both the protein total copy number as well as the total sequence coverage obtained for the protein. The tryptic peptide containing the K28 modification is identical in at

least 3 different human histone proteins annotated in SwissProt UniProt database today, all of which exist in excess of one million copies in most mammalian cells.[11]
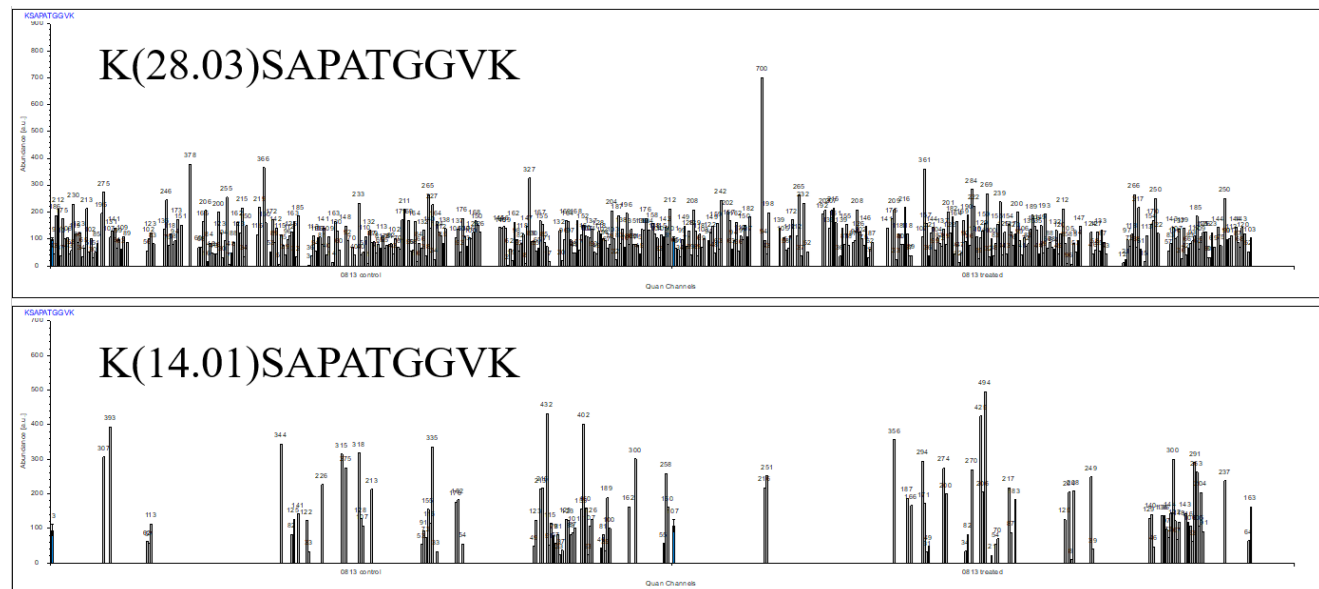
Figure 2. The measured abundance of two PTMs on histone 3 with 580 single 0813 cells shown. Top, the K28 dimethylated peptide was observed in over 75.8% of these cells. A single dimethylation on this lysine was observed less frequently. PTMs on K28 were observed in 98.7% (573/580) of all single 0813 cells in this analysis.

Unsupervised analysis can discriminate between similar pancreatic cancer cell lines

One quality control metric for a single cell proteomics methods that has been employed by multiple groups is the demonstration of cell type clustering by unsupervised statistics such as PCA.[12–14] If HeLa cells and HEK293 cells form distinct clusters when analyzed together, it stands to reason that the method is sound. One criticism of this method is that there are considerable differences between the size and protein content of these two common laboratory cancer cell line strains. ASPC-1 and PANC 0813 are two highly similar pancreatic cancer cell lines that were derived from patient samples in a similar way.[15] In addition, both cell lines possess two copies of the KRAS[G12D] mutant gene. One major difference is that the ATCC recommends supplementing media for growing PANC 0813 with insulin, where none is recommended for ASPC-1. As shown in **Figure 3A**, a simple principal component analysis can entirely resolve these two cancer cell lines when in excess of 200 cells per condition. A recent preprint demonstrated that the largest proteomic effects in single cell measurements are simply cell size and recommended the normalization of single cell signal using histones as a metric.[16] While normalization with Histone H4 does appear to reduce the differences between these two cell lines, they largely cluster independently by PCA (**Figure 3B**).
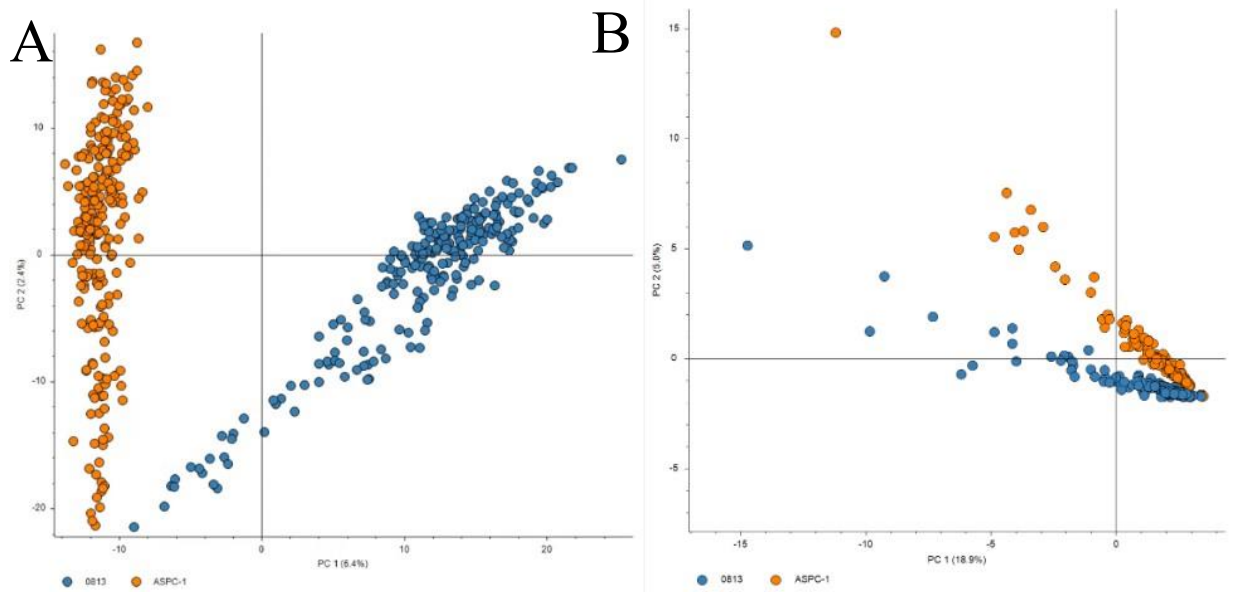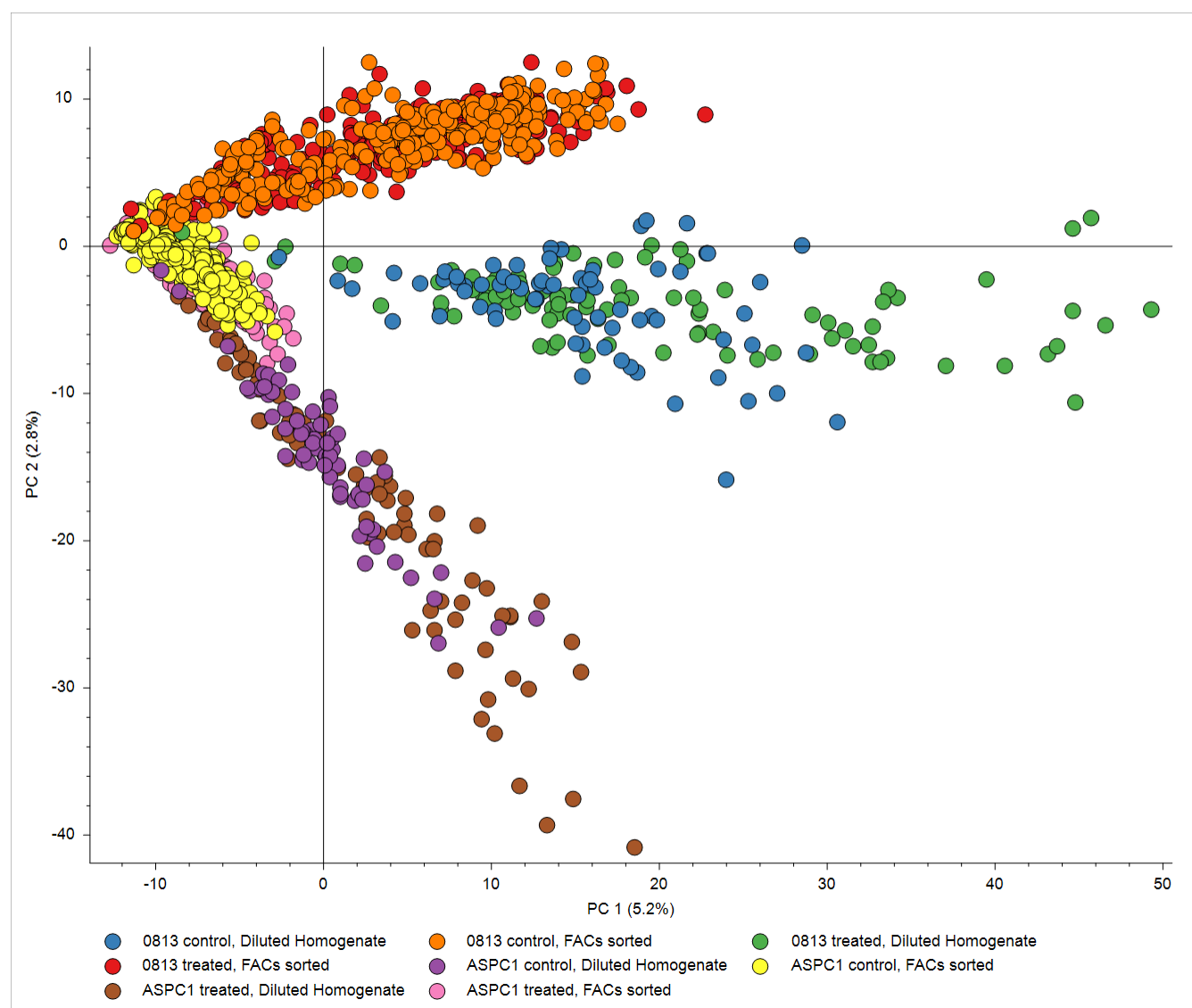
Figure 3. Principal component analysis of random injections of two similarly derived KRAS[G12D] mutant pancreatic cancer cell lines. PANC0813 (blue) and ASPC-1 (orange) both harbor two copies of the KRAS[G12D] mutation and were derived from pancreatic ascites through passage in a xenograft model. Despite this projected similarity they cluster independently in this analysis. **A.** Normalization to the total PSM level abundance in each cell line. **B.** Normalization to the peptide signal of Histone H4.

How carrier channels are prepared alters the proteins that can be detected in SCoPE-MS

There are two main strategies today for the preparation of carrier channels for multiplexed SCP. The original study by Budnik *et al*., utilized a collection of single cells which were lysed and prepared as the carrier channel.[14,17–19] Studies utilizing the advanced liquid handling devices such as the CellenOne system, a miniaturized robotics system based on the SciFlex Arrayer[20], likewise use this strategy. In our recent work, we utilized prepared a bulk cell homogenate of cells to be analyzed, labeled that with the 134c channel and prepared a dilution series to obtain an ideal carrier for all cells.[6] To evaluate the differences between these two approaches, I prepared carrier channels for PANC 0813 and ASPC-1 using both approaches. As shown in **Figure 4** unsupervised analysis distinctly classifies the two groups in both cell lines even when the two cell lines are compared suggesting that this imparts as large of an effect as patient origin and cell media conditions.

Figure 4. Principal component analysis of ~1,800 KRAS^{G12D} homozygous cells treated with MRTX1133 visualizing pseudo-randomly isolated, labeled and injected single cells from control and treated cell lines. Experiments where the carrier channel was prepared from FACs isolated single cells are denoted as "FACs sorted". Experiments where the carrier was prepared from a bulk cell homogenate that was labeled and diluted are denotes as "Diluted Homogenate".

Carrier channels prepared from bulk cell lysates demonstrate higher representation of cell death related proteins

To assess the differences imparted by the two carrier channel preparation strategies, I examined the functions of proteins exclusively identified in each carrier channel experiment. Venny [21] was used to identify proteins unique to each condition in PANC 0813 and ASPC-1 control and treated cells and proteins unique to each group were evaluated with StringDB.[22] While the largest differences observed appeared to be linked to mitochondrial function (data not shown) caspase proteins appeared to be differential between the two experiments. Manual evaluation of the original proteomic data confirmed that both

Caspase 6 and Caspase 8 were only detected in experiments where the carrier channel was made from a bulk cell homogenate rather than FACS isolated cells with intact cellular membranes. Likewise, TRADD, a regular of cellular apoptosis was only detected in single cells when a bulk cell homogenate was used for a carrier channel (**Supplemental Figure 3**).

The single cell proteomics does not recapitulate the bulk proteomic findings

As mentioned above, MRTX1133 treatment at this time point leads to a decrease in MAPK pathway protein levels, in particular a notable 2-5x decrease in MAPK3 (ERK) protein levels in bulk cell lysates. In no experiment with PANC 0813 or ASPC1 single cells did I note comparable decrease in ERK levels following drug treatment when using sum PSM level normalization. Similarly, I do not observe any quantitatively significant decrease in the Rho pathway, nor in the MHC protein expression machinery. This is despite relatively high relative coverage of these proteins in single cells. In addition, plus-minus detection metrics commonly used in single cell transcriptomics do not suggest there is an alteration in these lines following treatment. MAPK1, for example, was identified in 61.4% of 0813 single cells and in 61.6% of 0813 treated cells in this study.

While the root cause of this discrepancy appears impossible to discern in this current study, three main conclusions come to mind. The first is that we may have overestimated the quantitative accuracy of this approach. While we have shown that we can observe significant protein level alterations in diluted protein standards, it is possible that in the face of actual single cell biological and technical variability, these ratios disappear into the error bars. The second is that normalization to the total peptide abundance or histone signal are incorrect methods for dealing with single cell data in this manner. A third possibility is by sorting for viable cells we may place an intrinsic bias in our cells that removes our cells of. Single cell aliquoting on a FACs instrument uses multiple gating parameters prior to aliquoting and this may eliminate the cells that are responding to drug treatment.
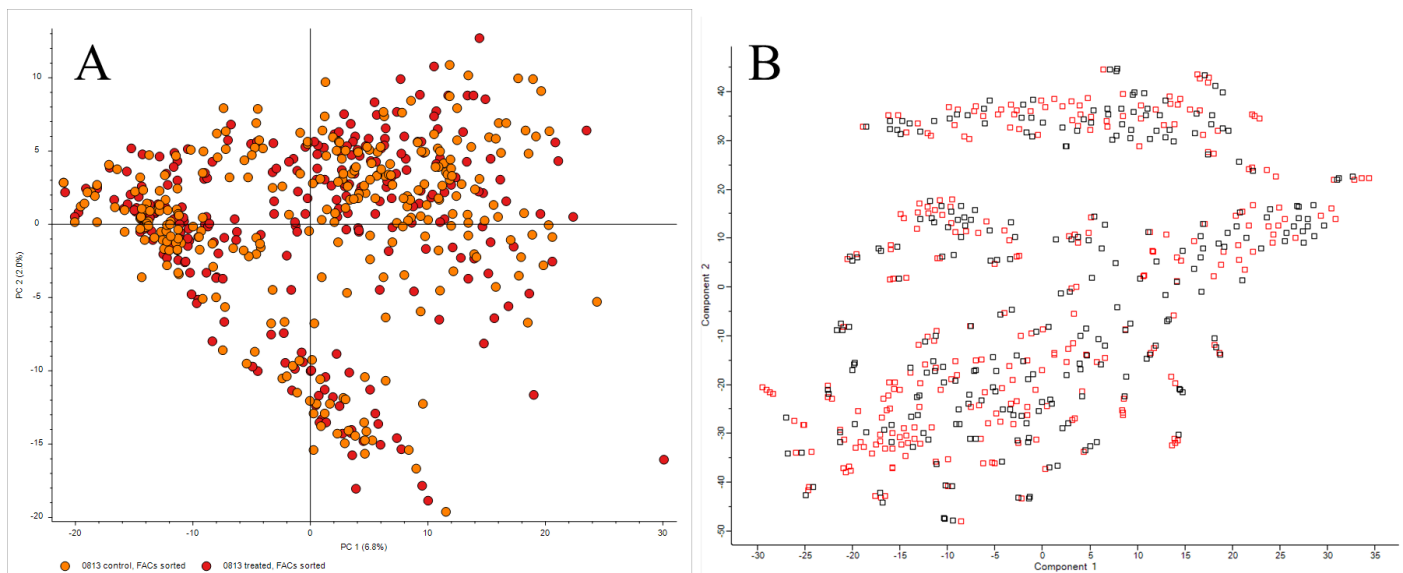

Figure 5. Control and treated PANC 0813 cells cannot be differentiated by unsupervised analysis. A. A principal component analysis of control and MRTX 1133 treated cells shows no distinct clustering. **B.** A UMAP analysis of the same cells demonstrates the same lack of resolution between single cells.

Even reduced carrier proteome effects may limit our ability to quantify relatively small changes in protein signal

In our recent work we used a two proteome standard to attempt to determine the limits of quantitative accuracy of pasefRiQ for single cell proteomics.[6] While we observed ratio compression while using increased carrier channels, these appeared to be significantly less than those observed on Orbitrap instruments. At approximately 200x carrier we observed that known ratios of 5:1 were reduced to approximately 3:1. A simple linear extrapolation on these ratios on a ratio of 2:1 would suggest a 60% ratio suppression rate. In the bulk proteomics of the PANC 0813 line we see a 2.38-fold decrease in MAPK3 and a 3.46-fold decrease of the same in ASPC-1 following MRTX1133 acute treatment. At a 60% ratio compression rate, PANC 0813 MAPK3 expression would represent only a 1.48-fold decrease and ASPC1 would demonstrate at 2.08-fold. In addition, serial dilutions of commercially prepared standard lysates are nice to optimize on but do not reflect true single cell variability or technical variation.

In cases where drug treatment may result in large cell death, sorting may result in heavily biased results

PANC 0203 and PANC 0304 have been recently described as two cell lines with extremely high sensitivity to MRTX1133.[5] My results strongly support these claims as 10 nanomolar treatment for 48 hours resulted in both dramatic reductions in viability as well as alteration in cellular morphology as detected by fluorescence scatter. During single cell isolation, viable cells are collected based on scatter using a nuclear stain that cannot cross intact cell membranes to help eliminate damaged or dead cells. For both PANC 0203 and PANC 0304 cells it was not possible to collect 200 cells for the carrier channel for all of the intended plates due to the reduced number of cells and altered morphology of the viable cells. Sorting gates required adjustment for both treated cell lines due to the level of difference in relative scatter compared to control (**Figure 6**). In this case, the cells that were isolated appeared to be the minority of all cells and there were concerns as to the biological value of these cells in this study.
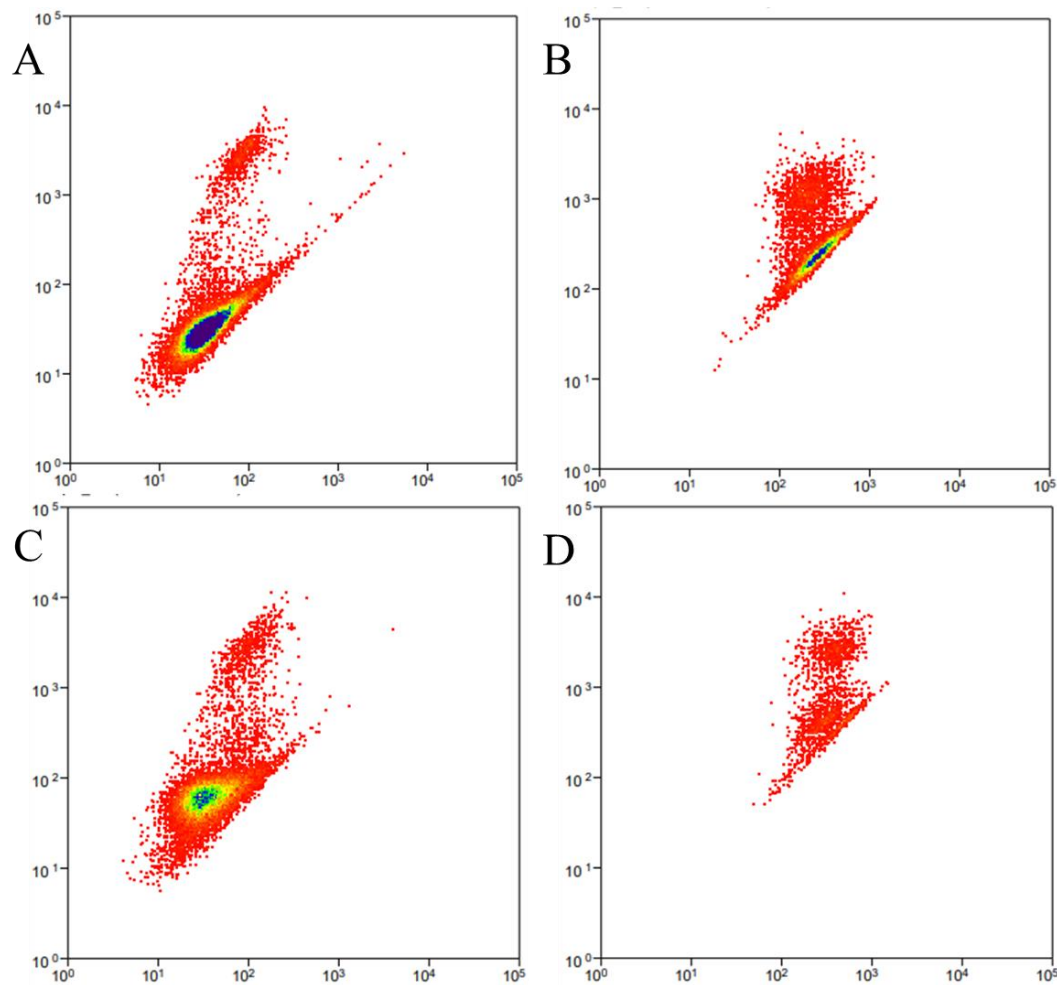
Figure 6. Fluorescence output data for two KRASG12 mutant cell lines following acute treatment with MRTX1133. A. ASPC-1 control cells. **B**. ASPC-1 treated cells. **C.** PANC 0203 control cells. **D.** PANC 0203 cells treated with MRTX1133.

Limitations of this current study

Considerable limitations exist in this current work as described. Limitations in the metabolomics analysis include the lack of internal or external controls for the identification and relative quantification of the identified metabolites. All identifications were made through a combination of high resolution MS1 and MS/MS identifications against spectral library databases. As no tools have been fully implemented today for the estimation and false discovery rates of metabolomics data today library matches should always be interpreted with caution. Similarly, the bulk proteomics data provided was largely generated using the default instrument parameters for diaPASEF provided in TIMSControl 4.0 and Compass 2023. While a comparison of different methods for diaPASEF are far outside the scope of this current work, our group has observed considerable increases in protein and peptide identifications following this software upgrade. Likewise, interpretation of these data was performed with SpectroNaut 17 which was new to our group prior to this study. We again observe considerable increases in peptide identifications versus previous versions and these results have not been thoroughly evaluated by our team or in published work to date.

Specific limitations of the single cell proteomics data described herein

It is hard to know where to even start with the myriad of limitations in single cell proteomic studies today, and there are particularly glaring limitations in this study I've described. Although I attempted to isolate and analyze 4,000 single cells, only a little more than 45% of these were deposited on the MASSIVE repository. The striking amount of cell death and morphological alterations in PANC 0203 and PANC 0304 cells following treatment restricted my ability to obtain cells for treated loading channels. As such, my carrier channel load was decreased from approximately 40 nanograms to 20 nanograms due to the absence of treated cells. While this does not appear significant in the face of the increasing sensitivity of mass analyzers today this method has been optimized for higher relative carried loads. The TIMSTOF Flex instrument is not only multiple generations old, but this device is used in our lab extensively for imaging and bulk cell proteomic analysis. Under ideal circumstances, perhaps a dedicated instrument would be used that could be maintained for the maximum possible cleanliness and overall sensitivity. However, in our working environment these factors together mean a 20ng total peptide load causes a considerable decrease in peptide and protein identification rates in this experiment. More importantly, since the SCoPE-MS method relies largely on the identification of peptides that are present in the carrier channel, the lack of treated cells in the carrier channel can lead to heavy biases in the data. For example, proteins that are of increased abundance following drug treatment may not be detected at all or under-represented as the only peptides "amplified" by the carrier channel are the ones in the control cells. The inverse is also true in that proteins that are of increased relative abundance in control cells are now over-represented in the single cell data. While the analysis of this effect is light years beyond the scope of this current study it has led me to eliminate these two cell lines from this current draft of the study. In addition, although I have used a considerably lower carrier channel than in our previous study, the impurities from the TMT label of the carrier channel (135) do impart considerable inflation on the 134 single cell channel. Therefore, the cells labeled with this channel should be disregarded in this study. Finally, this study is largely a pressure test to determine the challenges and limitations of large scale implementation of this approach in a pharmacological model. A thorough analysis of dosing conditions for each cell line will be necessary to truly apply this approach as a relevant tool in the analysis of the effects of MRTX 1133 in multiple cancer cell lines. This is work that is currently underway.

Conclusions

In this work I describe the application of metabolomics, proteomics and single cell proteomics to the analysis of acute dosage of a promising new small molecule inhibitor. While MRTX1133 is currently in clinical trials and may not succeed, it is inevitably the basis of further compounds to target one of the most deleterious of all human cancer mutations.[23] Metabolomic analysis demonstrates that the drug leads to a decrease in both ATP and NAD precursors in all cell lines. In addition, glutamine levels appear to be affect cells differently based on the number of copies of the mutant form in these cell lines. However, this is the result of only four cancer cell lines and these results should be interpreted with caution. Proteomic analysis indicates the expected decrease in the MAPK pathway in all cell lines as well as an alteration in GTPase signaling and MHC expression as a whole. In general, results that should be expected based on previous results.[1,24] To add further granularity I performed multiplexed single cell proteomics on these four cell lines with an aim of completing an analysis of 4,000 single human cells. Due to the high level of death and morphological alterations in the cell lines harboring single mutant copies, it was not possible to obtain enough cells for construction of carrier channels and I chose to disregard the results from two

cell lines. Label free single cell proteomics will be performed on these cell lines and work has begun in this direction.

The loss of viability of the single copy mutant cell lines suggests some new concerns in applying single cell proteomics in drug treatment studies. Is cellular viability a correct criterion for the aliquoting of single cells when drugs are used which may result in high numbers of dead cells?

These concerns can be further extended to even treatments where the number of dead cells does not appear significantly higher than control cells. When cells are collected for carrier channels based on the presence of an intact cell membrane that does not permit propidium iodide staining, this imparts biases compared to bulk cell lysate carrier channels where living and dead cells may be homogenized. While many of the protein level differences between cells analyzed with the two carrier channel strategies are difficult to reason through, some are not. The presence of Caspases 6 and 8 and the apoptosis regulator TRADD were exclusively detected in single cells where a bulk cell lysate carrier channel was employed. This strongly suggests that when FACs isolates viable cells as carrier channels, proteins from cells that are dead or dying are not being equally assessed in both experimental designs. In the case of drugs such as MRTX1133 where the ultimate goal is the death of cells harboring a specific mutation, it is unclear to me how to counter for these biases to better understand drug activity and resistance. The most challenging question of all, however, is in how this may affect standard proteomics of bulk cell lysates when populations of cells clearly exist in at least two states, viable or unviable following drug treatment.

Considerable effort today is being directed toward the improvement of the field of single cell proteomics. The majority of work has centered on developing new methods for cellular isolation, peptide recovery, and instrument methods.[14,25–27] However, a recent multi-institute collaborative effort has provided suggestions for the reporting of single cell proteomics data.[28] Informatics continues to develop as well to address the unique challenges inherent in this emerging new field.[29,30] Equal effort may be necessary to identify the parameters for a successful experimental design in the case of drug treatment models. If this study only succeeds in providing a relatively large dataset into the open domain for potential reanalysis and for pressure testing new informatics, I consider this a holiday break well spent.

Methods

Cell culture and drug treatment

All cell lines were obtained from ATCC between March and December of 2022. All cell lines were cultured according to vendor instructions using cell culture media purchased from the vendor for this purpose. PANC 0813 requires supplementation with insulin, and this was purchased from Fisher Scientific through the JHU Core store. All cell lines were passaged a minimum of 3 times prior to treatment with 10 nanomolar MRTX1133 for 48 hours. Cells were harvested according to ATCC vendor instructions. Briefly, the cell culture media from each flask of cells was aspirated and the cells were briefly rinsed in 3 mil of the recommended Trypsin EDTA solution from ATCC. This solution was rapidly aspirated off and replaced with 3 mL of the same solution. The cells were examined by light field microscopy and incubated at 37°C with multiple examinations until the adherent cells had lifted off of the plate surface. The active trypsin was then quenched by addition of 7 mL of the original culture media. The 10 mL solution was placed into sterile 15 mL falcon tubes and centrifuged at 300 x g for 3 minutes to concentrate the cells. The

supernatant was gently aspirated off and the cells were resuspended in PBS solution without calcium or magnesium with 0.1% BSA (both, Fisher Scientific) at an estimated 1 million cells per mL as estimated by bright field microscopy. Approximately 2 million cells were taken for bulk proteomic and metabolomic analysis. Cells for single cell aliquoting were gently dissociated from clumps by slowly pipetting a solution of approximately 1 million cells through a Falcon cell strainer (Fisher, 353420) and the cells were placed on wet ice and immediately transported across the street to the JHU Public Health sorting core. Non-viable cells were labeled with a propidium iodide solution provided by the core facility and briefly vortexed prior to cell isolation and aliquoting.

Global Metabolomics

A solution containing approximately one million cells from each condition was centrifuged at 13,000 *x g* for 15 seconds at speed to obtain a solid pellet. The solution was aspirated off and replaced with 300 microliters of 70% methanol solution. Pellets were resuspended with vigorous vortexing and placed at -80°C for approximately 2 days. Following storage, the cells and methanol solution were thawed on wet ice and resuspended with vigorous vortexing, followed by centrifugation at 13,000 *x g* for 5 minutes to precipitate proteins and cellular debris. The top 250 microliters of supernatant was removed to limit disturbing of the lower material and was dried to completeness via SpeedVac at 25°C. The dried metabolite extract was resuspended in 50 microliters of 5% acetonitrile 0.1% formic acid in LCMS grade water. Two microliters of solution were used for each replicate LCMS analysis. For LCMS analysis a Q Exactive "Classic" system coupled to Dionex U3000 UHPLC was used for all analysis. Separation was performed on a 2.1 mm x 15 cm HyperSil Gold Colum with 2 micron particle size and a flow rate of 300 microliters/minute for the active gradient. The LCMS method parameters have been deposited at www.LCMSmethods.org as "Q Exactive Positive Metabolomics" in the 2019 method release. All resulting output files were processed in Compound Discoverer 3.1 using a combination of 3 human metabolite libraries from mzCloud, ChemSpider, and a local desktop library of 4,000 human metabolites provided by Thermo Scientific. Compound identities were prioritized in the case of conflict between databases in the order described above.

Bulk proteomics

A solution containing approximately one million cells from each condition was rapidly centrifuged at 13,000 *x g* for 60 seconds at speed to obtain a solid pellet. The sorting solution was carefully aspirated off and the cell pellet was replaced with 200 microliters of S-Trap lysis buffer (5% SDS in 100mM TEAB, ProtiFi). The pellet was suspended with rigorous vortexing prior to being placed in an ultrasonic water bath for 15 minutes at 37°C for further cellular lysis. Fifty microliters of each sample was taken for reduction at 95°C for 5 minutes in 20mM DTT followed by benchtop cooling to room temperature and alkylation with 30mM iodoacetamide for 20 minutes at room temperature in a light tight drawer. Pierce "Easy Aliquot" single use reagents were used for both reduction and alkylation. Another 50 microliters of each solution were taken for digestion without reduction and alkylation for the later construction of bulk cell digest carrier channels.

All proteomic analysis was performed on a TIMSTOF Flex mass analyzer coupled to an EasyNLC 1200 system (Proxeon) by a 15 cm x 75 micron PepSep column with 1.9 micron Reprosil particles. The data acquisition method was the default diaPASEF method "short gradient diaPASEF" included in TIMS Control 4.0 2023. The chromatography gradient ramped from 8% buffer B (80% acetonitrile in 0.1% formic acid) to 35% B in 25 minutes with a flow rate of 350nL/min prior to a rapid increase to 100% B at 500 nL/min

by 30 minutes. Baseline conditions were restored at the beginning of each chromatography gradient by the EasyNLC prior to sample loading.

Single cell aliquoting

Single cell proteomics sample preparation, analysis and data processing were performed as described previously.[6] Briefly, single cells were aliquoted using an analog MoFlo sorter into cold 96 well plates containing 2 microliters of LCMS grade acetonitrile. At the completion of each plate aliquoting they were immediately sealed and placed in an insulated box of dry ice with the wells pressed into the material to ensure rapid cooling. Due to the size of this study and the difficulty of transporting multiple boxes of dry ice across a busy city street late at night in the winter, after approximately 5 minutes, each plate was transferred to a cooler of wet ice for transport back to our lab and -80⁰C storage. Estimations of cellular viability and cell aliquoting efficiency were provided by the operator who has over 30 years of cell sorting and aliquoting experience. Digital reports were provided by email following the sort and are available upon request.

Single cell lysis, digestion and combination of multiplexed cells

Single cells were placed into storage followed extensive use of tape to help ensure plate seal integrity during storage. A full protocol describing all steps of cell lysis, digestion and TMT labeling is provided on Protocols.io through the LCMSmethods.org initiative and can be accessed at the following **dx.doi.org/10.17504/protocols.io.yxmvm2w16g3p/v1**. Cell lysis was further driven to completeness and acetonitrile was removed by placing each plate directly from cold storage onto a 95⁰C hot plate for approximately 90 second. The plates were cooled to room temperature on a benchtop with static free surface covers. The author performed all aliquoting of reagents while standing on a static free floor mat for all stages of the preparation. Periodically a Zero Stat "static gun" clearly labeled in fluorescent pink tape "NOT A GUN" repeatedly to help ensure author survival during late night sample preparation was used on plates to further minimize the negative side effects of static electricity on single cells (Fisher Scientific, NC9663078). Dried lysed cellular lysate was digested using a solution of 5 nanogram/microliter LCMS grade trypsin (Pierce) in 0.1% n-Dodecyl-beta-Maltoside Detergent (DDM, Thermo Fisher, 89902). One microliter of trypsin solution was used for all single cells and blank wells and four microliters were used for digestion of the carrier channel lanes. The excess trypsin was used as an extension of the "sacrificial carrier" concept recently described in Choi *et al.*,.[31] The plates were tightly sealed and incubated for 2 hours at 45⁰C in an Orbital shaker with centrifugation every 30 minutes to concentrate condensing liquid. Following digestion, the plates were cooled to room temperature and centrifuged again to precipitate all liquid solution. TMT Pro 18 reagents previously prepared and aliquoted at a concentration of 20 nanograms per microliter were used to label all wells and sacrificial trypsin peptides by adding 1 microliter and incubating for 30 minutes at room temperature with orbital shaking. A solution of 0.5% hydroxylamine in TEAB was used to quench remaining TMT by adding 0.5 microliters to each single cell and blank well and 2 microliters to each carrier channel well along with a 20 minute incubation at room temperature with orbital shaking. Each plate was then dried by SpeedVac at room temperature, which took approximately 5 minutes for each 4 plates. The ten unit resolution TMT channels from the TMTPro 18 kits (Thermo Fisher) with channels alternated to minimize isobaric carrier impurities and interference.[32] TMT labeled single cells and carrier channels were combined in a staggered manner in which each TMT plex contained a mixture of the control and treated carrier channel digest and control and treated wells. This is best described using the illustrations in the protocols.io repository

(**dx.doi.org/10.17504/protocols.io.yxmvm2w16g3p/v1**). The net result is that each well in the autosampler plate contains a carrier channel that is an equal mixture of control and treated cells. In addition four cells from control and four cells from treated cells independently labeled and measured in each LCMS experiment. By staggering the plates, we can obtain a pseudo-random injection pattern where a different set of single cells from each batch with alternating labels are injected consecutively. The TMT channel identities are deconvoluted during the final data analysis.

Single cell data analysis

As previously described,[33] I utilize a single point recalibration method using the 135n carrier channel signal to adjust the reporter ion region. This secondary calibration allows tighter mass accuracy tolerances to be used during the final data analysis, resulting in reduced ion noise. For all ASPC-1 and PANC 0813 cells to meet the QC requirements for inclusion in this manuscript, the linear calibration shift applied was +0.0141 Da. This was performed using an updated version of the pasefRiQ calibrator with a GUI interface and the ability to batch recalibrate MGF files. This software is openly available and permanently published at DOI: 10.5281/zenodo.7259511**.** The recalibrated output files were processed in Proteome Discoverer 2.4SP1 using SequestHT and Percolator. Briefly, the MS/MS spectra were binned into 100 Da segments and filtered so that only the top 12 most abundant ions from each bin were retained. The resulting cleaned spectra were searched with a 15ppm MS1 tolerance and 0.03 Da MS/MS tolerance. TMTPro labels were considered static on the N-terminus and dynamic on lysines to allow for the search for lysine acetylation, methylations and dimethylation. Methionine oxidation was the only additional dynamic modification. The default cutoffs for Percolator PSM validation and peptide and protein FDR determination were employed in all analyses. Reporter ions were integrated using a 35ppm mass tolerance window (17.5 ppm up and down) and quantification was only used for unique proteins. Multiple consensus workflows were performed on the resulting MSF files to assess different normalization methods. The final data report for downstream analysis used a sum based normalization of all PSM signal for TMTPro channels 127-133. The 134 single cell channel was discarded in all runs due to apparent inflation from impurities in the 135 reagent channel.

Blank and carry over estimation.

The D.I.D.A.R.S.C.P.Q.C. program recently described was used to quantify the number of spectra in each recalibrated file that contained a quantifiable signal for each reporter ion used in this study. The diagnostic ions counted were 126.1277, 127.1248, 128.1344, 129.1314, 130.1411, 131.1382, 132.1479, and 133.149. Spectra containing ions within 0.005 Da of these masses (0.002.5 above or below) were simply counted. At this point no signal cutoff is employed.

Uniform Manifold Approximation and Projection (UMAP)

The normalized output sheet for all single cells from Proteome Discoverer was converted to .CSV and loaded into Perseus 1.6.17.[34] Perseus was previously set up to communicate with R 4.1.3 as described previously.[10] All single cell channels were added into Perseus as "Main" data points with the Protein Accession and Description added as "Text" variables. All zero datapoints were replaced with normal distributions with each single cell used as the distribution matrix individually. The cells were then grouped under row categories describing their individual cell and dose conditions. UMAPs were generated using the default settings for Euclidean distribution with 15 neighbors, 2 components, random state of 1 and a minimum distance of 0.1. The output was plotted using the multi-scatter node in Perseus.

Data Availability

All proteomics data can be viewed in an interactive cloud-based database. The cell lines with a single and double copy of the KRAS^{G12D} mutant form were processed separately. The 0813 and ASPC-1 proteomics data can be found here: https://simplifi.protifi.com/#/p/4fd12e70-9809-11ed-b0f0-03f62ebcf0cd. The single copy mutant lines PANC 0203 and PANC 0304 can be found here: https://simplifi.protifi.com/#/p/28a07700-b93a-11ed-92f4-b7d04df347c4. The original RAW and processed files are divided between 3 openly available repositories at www.Massive.UCSD.edu: PXD039597, PXD039601 and PXD039600.

(1)   Santana-Codina, N.; Chandhoke, A. S.; Yu, Q.; Małachowska, B.; Kuljanin, M.; Gikandi, A.; Stańczak, M.; Gableske, S.; Jedrychowski, M. P.; Scott, D. A.; Aguirre, A. J.; Fendler, W.; Gray, N. S.; Mancias, J. D. Defining and Targeting Adaptations to Oncogenic KRASG12C Inhibition Using Quantitative Temporal Proteomics. *Cell Rep.* **2020**.

(2)   Hata, A. N.; Shaw, A. T. Resistance Looms for KRASG12C Inhibitors. *Nature Medicine*. 2020.

(3)   Wang, X.; Allen, S.; Blake, J. F.; Bowcut, V.; Briere, D. M.; Calinisan, A.; Dahlke, J. R.; Fell, J. B.; Fischer, J. P.; Gunn, R. J.; Hallin, J.; Laguer, J.; Lawson, J. D.; Medwid, J.; Newhouse, B.; Nguyen, P.; O'Leary, J. M.; Olson, P.; Pajk, S.; Rahbaek, L.; Rodriguez, M.; Smith, C. R.; Tang, T. P.; Thomas, N. C.; Vanderpool, D.; Vigers, G. P.; Christensen, J. G.; Marx, M. A. Identification of MRTX1133, a Noncovalent, Potent, and Selective KRASG12D Inhibitor. *J. Med. Chem.* **2022**, *65* (4), 3123–3133.

(4)   The KRASG12D Inhibitor MRTX1133 Elucidates KRAS-Mediated Oncogenesis. *Nat. Med.* **2022**, *28* (10), 2017–2018.

(5)   Hallin, J.; Bowcut, V.; Calinisan, A.; Briere, D. M.; Hargis, L.; Engstrom, L. D.; Laguer, J.; Medwid, J.; Vanderpool, D.; Lifset, E.; Trinh, D.; Hoffman, N.; Wang, X.; David Lawson, J.; Gunn, R. J.; Smith, C. R.; Thomas, N. C.; Martinson, M.; Bergstrom, A.; Sullivan, F.; Bouhana, K.; Winski, S.; He, L.; Fernandez-Banet, J.; Pavlicek, A.; Haling, J. R.; Rahbaek, L.; Marx, M. A.; Olson, P.; Christensen, J. G. Anti-Tumor Efficacy of a Potent and Selective Non-Covalent KRASG12D Inhibitor. *Nat. Med.* **2022**, *28* (10), 2171–2182.

(6)   Orsburn, B. C.; Yuan, Y.; Bumpus, N. N. Insights into Protein Post-Translational Modification Landscapes of Individual Human Cells by Trapped Ion Mobility Time-of-Flight Mass Spectrometry. *Nat. Commun.* **2022**, *13* (1), 7246.

(7)   Pearlman, A. H.; Hwang, M. S.; Konig, M. F.; Hsiue, E. H.-C.; Douglass, J.; DiNapoli, S. R.; Mog, B. J.; Bettegowda, C.; Pardoll, D. M.; Gabelli, S. B.; Papadopoulos, N.; Kinzler, K. W.; Vogelstein, B.;

Zhou, S. Targeting Public Neoantigens for Cancer Immunotherapy. *Nat. Cancer* **2021**, *2* (5), 487–497.

(8) Kelstrup, C. D.; Aizikov, K.; Batth, T. S.; Kreutzman, A.; Grinfeld, D.; Lange, O.; Mourad, D.; Makarov, A.; Olsen, J. V. Limits for Resolving Tandem Mass Tag Reporter Ions with Identical Integer Mass Using Phase Constrained Spectrum Deconvolution. *bioRxiv*. 2018.

(9) Huffman, R. G.; Chen, A.; Specht, H.; Slavov, N. DO-MS: Data-Driven Optimization of Mass Spectrometry Methods. *J. Proteome Res.* **2019**.

(10) Yu, S.-H.; Ferretti, D.; Schessner, J. P.; Rudolph, J. D.; Borner, G. H. H.; Cox, J. Expanding the Perseus Software for Omics Data Analysis With Custom Plugins. *Curr. Protoc. Bioinforma.* **2020**, *71* (1), e105.

(11) Wiśniewski, J. R.; Hein, M. Y.; Cox, J.; Mann, M. A "Proteomic Ruler" for Protein Copy Number and Concentration Estimation without Spike-in Standards. *Mol. Cell. Proteomics* **2014**.

(12) Brunner, A.-D.; Thielert, M.; Vasilopoulou, C.; Ammar, C.; Coscia, F.; Mund, A.; Hoerning, O. B.; Bache, N.; Apalategui, A.; Lubeck, M.; Richter, S.; Fischer, D. S.; Raether, O.; Park, M. A.; Meier, F.; Theis, F. J.; Mann, M. Ultra-High Sensitivity Mass Spectrometry Quantifies Single-Cell Proteome Changes upon Perturbation. *Mol. Syst. Biol.* **2022**, *18* (3), e10798.

(13) Specht, H.; Emmott, E.; Petelski, A. A.; Huffman, R. G.; Perlman, D. H.; Serra, M.; Kharchenko, P.; Koller, A.; Slavov, N. Single-Cell Proteomic and Transcriptomic Analysis of Macrophage Heterogeneity Using SCoPE2. *Genome Biol.* **2021**, *22* (1), 50.

(14) Hartlmayr, D.; Ctortecka, C.; Seth, A.; Mendjan, S.; Tourniaire, G.; Mechtler, K. An Automated Workflow for Label-Free and Multiplexed Single Cell Proteomics Sample Preparation at Unprecedented Sensitivity. *bioRxiv* **2021**, 2021.04.14.439828.

(15) Zhang, L.; Zhou, W.; Velculescu, V. E.; Kern, S. E.; Hruban, R. H.; Hamilton, S. R.; Vogelstein, B.; Kinzler, K. W. Gene Expression Profiles in Normal and Cancer Cells. *Science (80-.).* **1997**, *276* (5316), 1268–1272.

(16) Lanz, M. C.; Elias, J. E.; Skotheim, J. M. Cell Size Contributes to Single-Cell Proteome Variation. *bioRxiv* **2022**, 2022.10.17.512548.

(17) Budnik, B.; Levy, E.; Harmange, G.; Slavov, N. SCoPE-MS: Mass Spectrometry of Single Mammalian Cells Quantifies Proteome Heterogeneity during Cell Differentiation. *Genome Biol.* **2018**.

(18) Specht, H.; Harmange, G.; Perlman, D. H.; Emmott, E.; Niziolek, Z.; Budnik, B.; Slavov, N. Automated Sample Preparation for High-Throughput Single-Cell Proteomics. *bioRxiv* **2018**.

(19) Kelly, R.; Zhu, Y.; Liang, Y.; Cong, Y.; Piehowski, P.; Dou, M.; Zhao, R.; Qian, W.-J.; Burnum-Johnson, K.; Ansong, C. Single Cell Proteome Mapping of Tissue Heterogeneity Using Microfluidic Nanodroplet Sample Processing and Ultrasensitive LC-MS. *J. Biomol. Tech.* **2019**, *30* (Suppl), S61–S61.

(20) Löhr, K.; Borovinskaya, O.; Tourniaire, G.; Panne, U.; Jakubowski, N. Arraying of Single Cells for Quantitative High Throughput Laser Ablation ICP-TOF-MS. *Anal. Chem.* **2019**, *91* (18), 11520–11528.

(21)   Oliveros, J. C. *Venny. An interactive tool for comparing lists with Venn Diagrams*. BioinfoGP of CNB-CSIC.

(22)   Szklarczyk, D.; Morris, J. H.; Cook, H.; Kuhn, M.; Wyder, S.; Simonovic, M.; Santos, A.; Doncheva, N. T.; Roth, A.; Bork, P.; Jensen, L. J.; von Mering, C. The STRING Database in 2017: Quality-Controlled Protein–Protein Association Networks, Made Broadly Accessible. *Nucleic Acids Res.* **2017**, *45* (D1), D362–D368.

(23)   Drosten, M.; Barbacid, M. Targeting the MAPK Pathway in KRAS-Driven Tumors. *Cancer Cell*. 2020.

(24)   Xue, J. Y.; Zhao, Y.; Aronowitz, J.; Mai, T. T.; Vides, A.; Qeriqi, B.; Kim, D.; Li, C.; de Stanchina, E.; Mazutis, L.; Risso, D.; Lito, P. Rapid Non-Uniform Adaptation to Conformation-Specific KRAS(G12C) Inhibition. *Nature* **2020**.

(25)   Specht, H.; Emmott, E.; Petelski, A. A.; Gray Huffman, R.; Perlman, D. H.; Serra, M.; Kharchenko, P.; Koller, A.; Slavov, N. Single-Cell Mass-Spectrometry Quantifies the Emergence of Macrophage Heterogeneity. *bioRxiv*. 2019.

(26)   Schoof, E. M.; Furtwängler, B.; Üresin, N.; Rapin, N.; Savickas, S.; Gentil, C.; Lechman, E.; Keller, U. auf dem; Dick, J. E.; Porse, B. T. Quantitative Single-Cell Proteomics as a Tool to Characterize Cellular Hierarchies. *Nat. Commun.* **2021**, *12* (1), 3341.

(27)   Furtwängler, B.; Üresin, N.; Motamedchaboki, K.; Huguet, R.; Lopez-Ferrer, D.; Zabrouskov, V.; Porse, B. T.; Schoof, E. M. Real-Time Search-Assisted Acquisition on a Tribrid Mass Spectrometer Improves Coverage in Multiplexed Single-Cell Proteomics. *Mol. Cell. Proteomics* **2022**, *21* (4).

(28)   Gatto, L.; Aebersold, R.; Cox, J.; Demichev, V.; Derks, J.; Emmott, E.; Franks, A. M.; Ivanov, A. R.; Kelly, R. T.; Khoury, L.; Leduc, A.; MacCoss, M. J.; Nemes, P.; Perlman, D. H.; Petelski, A. A.; Rose, C. M.; Schoof, E. M.; Van Eyk, J.; Vanderaa, C.; Yates, J. R.; Slavov, N. Initial Recommendations for Performing, Benchmarking and Reporting Single-Cell Proteomics Experiments. *Nat. Methods* **2023**, *20* (3), 375–386.

(29)   Kalxdorf, M.; Müller, T.; Stegle, O.; Krijgsveld, J. IceR Improves Proteome Coverage and Data Completeness in Global and Single-Cell Proteomics. *Nat. Commun.* **2021**, *12* (1), 4787.

(30)   Vanderaa, C.; Gatto, L. Replication of Single-Cell Proteomics Data Reveals Important Computational Challenges. *bioRxiv* **2021**, 2021.04.12.439408.

(31)   Lombard-Banek, C.; Choi, S. B.; Nemes, P. Chapter Thirteen - Single-Cell Proteomics in Complex Tissues Using Microprobe Capillary Electrophoresis Mass Spectrometry. In *Enzyme Activity in Single Cells*; Allbritton, N. L., Kovarik, M. L. B. T.-M. in E., Eds.; Academic Press, 2019; Vol. 628, pp 263–292.

(32)   Brenes, A.; Hukelmann, J.; Bensaddek, D.; Lamond, A. I. Multibatch TMT Reveals False Positives, Batch Effects and Missing Values *. *Mol. Cell. Proteomics* **2019**, *18* (10), 1967–1980.

(33)   Orsburn, B. C.; Yuan, Y.; Bumpus, N. N. Insights into Protein Post-Translational Modification Landscapes of Individual Human Cells by Trapped Ion Mobility Time-of-Flight Mass Spectrometry. *Nat. Commun.* **2022**, *13* (1).

(34)   Tyanova, S.; Temu, T.; Sinitcyn, P.; Carlson, A.; Hein, M. Y.; Geiger, T.; Mann, M.; Cox, J. The Perseus Computational Platform for Comprehensive Analysis of (Prote)Omics Data. *Nat. Methods*

2016, *13* (9), 731–740.

Supplemental Figures
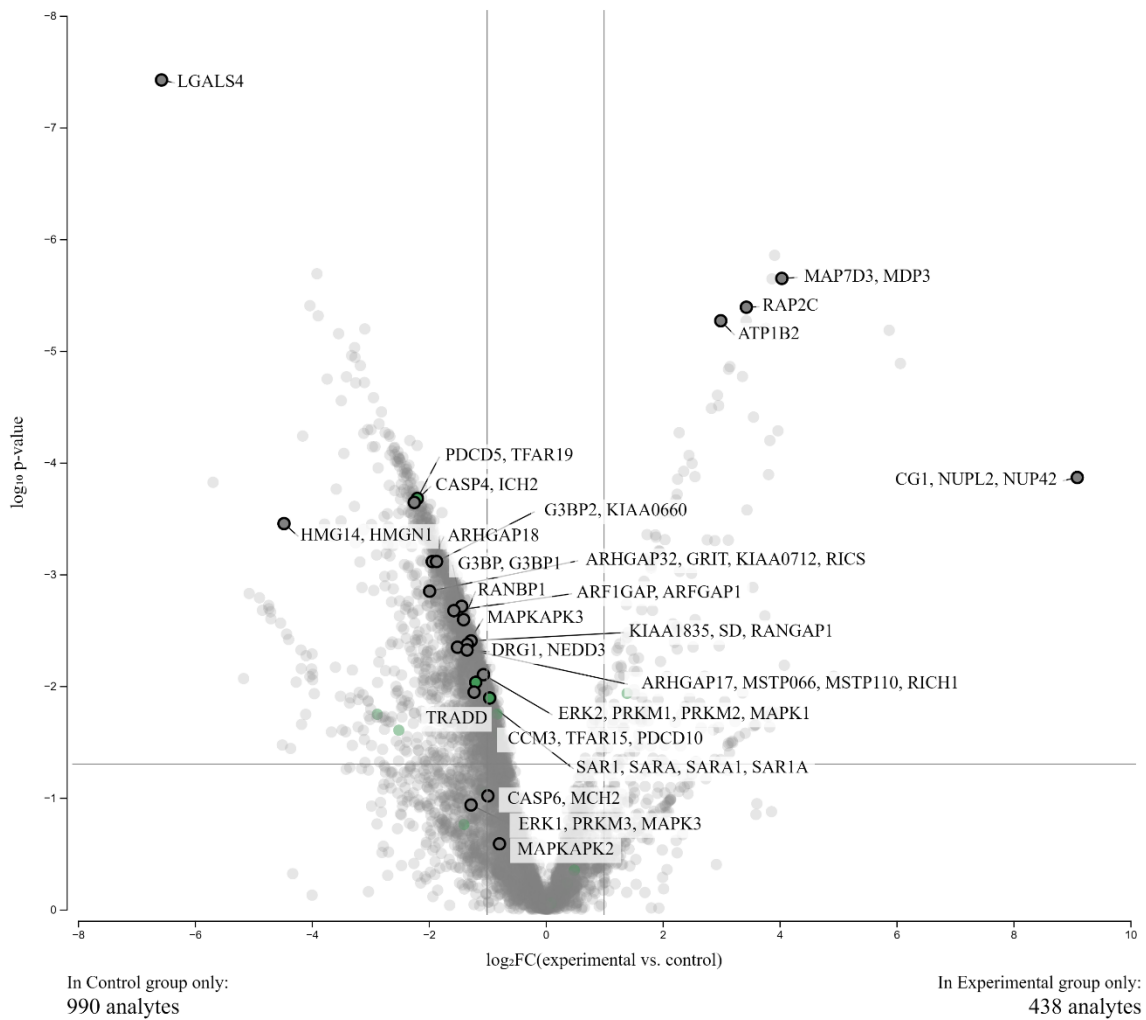
Supplemental Figure 1. A volcano plot generated by SimpliFi analysis of PANC 0813 control vs. treated.
Proteins specifically discussed in the manuscript have been manually highlighted for illustration.
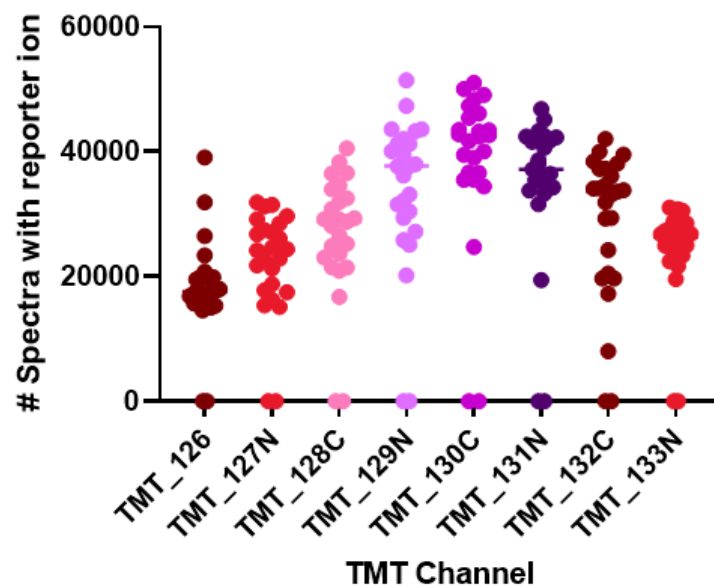
Supplemental Figure 2. The D.I.D.A.R.S.C.P.Q.C. output from one batch of PANC 0813 and ASPC-1 randomized control and treated cells.
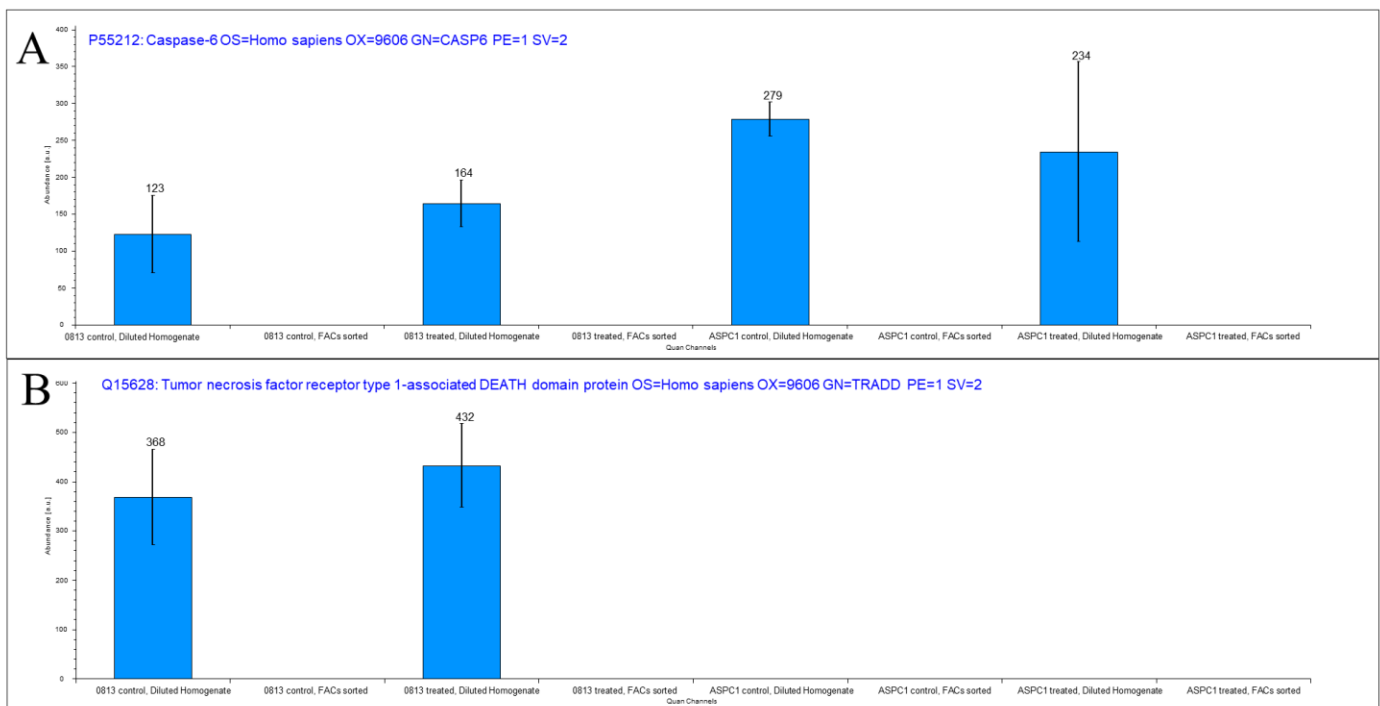
Supplemental Figure 3. The signal intensity of apoptosis related proteins between experiments. A. Caspase 6 is only detected in LCMS experiments where the carrier channel was constructed from a bulk cell lysate. **B.** Bar plot indicating that the TRADD apoptosis protein was only identified in PANC 0813 experiments where the carrier channel was constructed from a bulk cell lysate.